

SafeWind



Collaborative project funded by the European Commission
under the 7th Framework Program, Theme 2007-2.3.2:
Energy

“Multi-scale data assimilation, advanced wind modelling &
forecasting with emphasis to extreme weather situations
for a safe large-scale wind power integration”

Grant Agreement N°: 213740

Deliverable Dp9.5

“Guidelines and recommendations for wind prediction final users”

how smart consideration of meteorological aspects can promote wind power

DOCUMENT TYPE	Deliverable
DOCUMENT NAME:	swind.deliverable_Dp9.5.Guidelines_v2.1
VERSION:	V2.1
DATE:	2012.12.10
CLASSIFICATION:	R0: General public
STATUS:	Released

Abstract: This deliverable summarizes the findings of WP7 in terms of guidelines for using predictability during the planning phase of wind farm development. Methodologies for the assessment of wind power predictability at large and local scales are introduced with case studies to illustrate their practical use.

AUTHORS ¹ , REVIEWERS			
MAIN AUTHOR/EDITOR:	J. Sanz Rodrigo		
AFFILIATION:	CENER		
ADDRESS:	Calle Ciudad de la Innovación 7, 31621-Sarriguren, Spain		
TEL.:	+34 948 25 28 00		
EMAIL:	jsrodrigo@cener.com		
FURTHER AUTHORS:	L. Frías (CENER), N. Stoffels (UNIOL), L. von Bremen (UNIOL)		
PEER REVIEWERS:	G. Giebel (DTU)		
REVIEW APPROVAL:	Approved :		Rejected (improve as indicated below) :
SUGGESTED IMPROVEMENTS:			
APPROVER:			

VERSION HISTORY			
VERSION ² :	DATE:	COMMENTS, CHANGES, STATUS:	PERSON(S):
1.0	2012.07.23	First draft circulated to review and extract guidelines	J. Sanz Rodrigo (CENER)
2.0	2012.09.13	Complete draft sent for final review	J. Sanz Rodrigo (CENER)
2.1	2012.12.10	Final version including reviewer's comments	J. Sanz Rodrigo (CENER)

STATUS, CONFIDENTIALITY, ACCESSIBILITY							
STATUS:			CONFIDENTIALITY:			ACCESSIBILITY:	
S0	Approved/Released	X	R0	General public	X	Private web site	
S1	Reviewed		R1	Restricted to project members		Public web site	X
S2	Pending for review		R2	Restricted to European Commission		Paper copy	
S3	Draft for comments		R3	Restricted to WP members + PL			
S4	Under preparation		R4	Restricted to Task members +WPL+PL			

PL: Project leader **WPL:** Work package leader **TL:** Task leader

¹ The authors of this document are solely responsible for its content, which does not represent the opinion of the European Community and the European Community is not responsible for any use that might be made of data appearing therein.

² **VERSION NAMING :** V0.x draft before peer-review approval, V1.0 at the approval, V1.x minor revisions, V2.0 major revision

Contents

1.	Introduction.....	4
2.	Forecasting in the Planning Phase Considering End-user Needs	4
3.	European-wide Predictability Maps	6
3.1	Data.....	6
3.2	European Error Maps	8
3.3	Conclusions on large-scale predictability	11
4.	Wind Farm Predictability From Resource Assessment Campaigns.....	12
4.1	Methodology	12
4.2	Case Study.....	14
4.2.1	Wind climate changes between the planning and the operational phases	15
4.3	Model evaluation	16
4.3.1	Planning phase	16
4.3.2	Operational phase.....	16
4.4	Predictability assessment	17
4.5	Conclusions on local-scale predictability.....	19
5.	Guidelines for End-Users.....	20
6.	References	21

1. Introduction

An innovative aspect of the SAFEWIND project deals with the use of wind power predictability as a decision factor of the wind resource assessment phase, i.e. the integration of operational aspects of wind power prediction at an early stage when development issues are being considered. As a result, a more integrated vision of the value of wind energy throughout the live cycle of the development is possible and, in turn, wind power can be better promoted.

From site to regional/country and continental levels, wind power predictability is a relevant aspect for many stakeholders: TSOs (Transmission System Operators), policy makers, financiers, wind energy developers, operators and traders. Depending on the scale of the prediction, different forecasting products can be useful for the end-user.

The aim of this report is to produce guidelines on how to use predictability by stakeholders involved in the planning phase of wind energy. To this end, it is explained how to extract predictability information by generating virtual power production data at large (regional-EU) scale and at local (wind farm) scale. Two cases studies are presented in order to illustrate the methodologies: 1) predictability maps for Europe with evaluation focused in Germany and 2) wind farm predictability from three Spanish sites. The report is complementary to [Giebel and Kariniotakis \(2011\)](#), who describe best practice guidelines for the use of forecasting in the operational phase.

2. Forecasting in the Planning Phase Considering End-user Needs

In essence, these tools are basically the same used during the operational phase. An up-to-date review of wind power forecasting models can be found in [Giebel et al. \(2011\)](#) and [Foley et al. \(2012\)](#). The difference resides in the generation of virtual production data against which the prediction is made. Hence, forecasting models are used in hindcast mode, making use of historical data as a reference for future wind energy integration scenarios.

Production data is typically obtained from a power curve model that relates the wind speed of the site/area of interest with the power output, considering a reference wind turbine model. Hence, the resolution and accuracy of the model is directly linked with the representative scale of the input velocity. For instance, global analyses or reanalyses are produced with data assimilation systems that define the state of the atmosphere at resolutions of some tens to hundreds of kilometres at typically 3 to 6 hourly intervals. The spatial distribution of the wind speed can be translated to wind power to obtain a database of virtual production data representative of large regions. Then, Numerical Weather Prediction (NWP) models are used to produce forecasts from which the wind power predictability is obtained by comparison with the (re)analysis data. As a result, wind power predictability can be mapped over large regions and integrated in a Geographical Information System (GIS) together with other relevant geographical data. This enriched wind atlas can be used for life-cycle assessment of large-scale wind power integration studies. Policy makers or TSOs are the main beneficiaries of this kind of product.

If finer scales are relevant, it is necessary to make use of site measurements. Wind resource assessment measurement campaigns can be used together with a microscale model to produce virtual time series of production data. Then, wind farm forecast models are configured to assimilate this data as if they were real and site-level predictability can be evaluated. Together with a wind energy market model, this information can be added to the economical feasibility study of a wind farm project under development. Then, a wind energy developer or investor can produce estimates of the cost from lack of predictability during the lifetime of the wind farm.

Utilities are integrating more and more renewables in their energy mix. When it comes to buying wind energy projects to developers a clever spatial distribution of the power can imply important savings in terms of imbalance penalties from the energy market. While the annual energy yield constitutes the most important decision-making factor when buying wind power plants, it is nevertheless relevant to determine the costs due to lack of predictability and how they can be lowered by participating in the market with aggregations of wind farms. In effect, as the wind climate among the wind farm cluster is more uncorrelated, typically due to larger distances, temporal variability decreases and predictability increases due to spatial error smoothing. The correlation between forecast errors becomes weaker

with distance and the predictability of a region is always better than that of a single wind farm ([Focken et al., 2002](#)). This portfolio effect is also beneficial for the TSOs in reducing the balancing costs associated with reserves and congestion management. Hence, higher penetration of renewable energy generation is possible, reducing energy supply risks and lowering the electricity prices ([EWEA, 2009](#); [Rombauts et al., 2011](#)). The scenario of a pan-European grid is logically incentivized by this fact.

3. European-wide Predictability Maps

Wind power forecast errors strongly depend on the capacity factor which itself depends on the topography. To analyse the forecast errors in Europe, the COSMO-EU model from the German Weather Service DWD is utilized. The aim is to produce forecast error maps to characterise predictability for wind farms. Predictability can then be taken as criteria for developing new wind farms.

The generation pattern and the predictability of wind power play a key role to reach the ambitious goal of a renewable energy penetration of 80% in 2050 with respect to safe grid integration. While the weather cannot be influenced, the optimal spatial distribution of wind farm capacities can be estimated using historical data. The results can serve as input to political frameworks in order to promote wind energy in regions with optimal spatio-temporal wind power balancing characteristics.

3.1 Data

The COSMO-EU model by the German Weather Service (DWD) provides forecasts and analyses on a 4.1 x 7 km grid ([COSMO, 2011](#)). The domain has 735 x 625 grid points, hence 459,375 grid points in total. Forecasts are started at 00 UTC. Forecast steps 00 – 72 are used with an hourly resolution.

The presented data covers the year 2010. For the conversion from wind speed to wind power at 68.8 m height (model level 38) two different power curves are used. The TradeWind Power Curve ([McLean, 2008](#)) is used for the German TSO analysis while for the European forecast error maps a mean of two different power curves, namely: the Enercon E82 and the Vestas V90/2 (Figure 1).

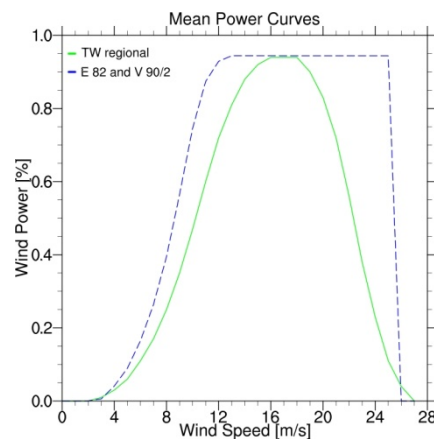


Figure 1: TradeWind power curve (green) and mean power curve (blue).

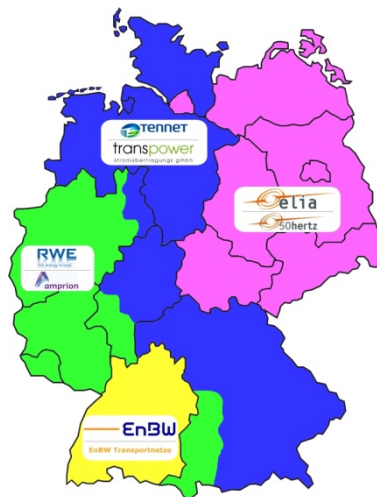


Figure 2: Map of the German TSO zones.

The question arises, if it is necessary to know the exact position of wind farms to get a good quantitative wind power forecast. To answer this question, a quantitative analysis of the forecast error in the German TSO zones is made. The TSO zones are presented in Figure 2.

Within the EnBW, 50Hertz and Amprion zone the wind farms are distributed quite homogeneous. Within the Tennet zone the majority of wind farms is concentrated in the northern part of Germany (Figure 3).

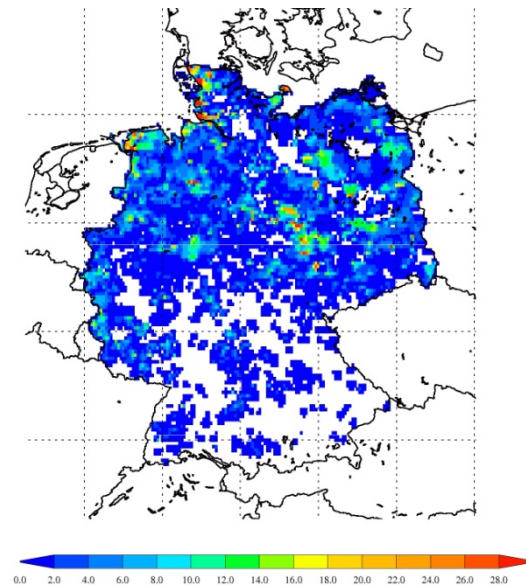


Figure 3: Distribution of the installed MW in Germany in January 2010.

In order to investigate the importance of the knowledge of the spatial distribution the TSO wind speed time series are converted into wind power at each grid point using the regional TradeWind power curve (Figure 1). In a first run, the assumption is made, that at each grid point, that holds wind power, the installed capacity is the same, i. e. in each zone the spatial distribution of wind power is homogenous. For the second run the actual distribution of wind power in each TSO zone (Figure 3) is taken to calculate the wind power.

In order to compare both distributions, the time series are bias corrected against the TSO measurements. These are real wind farm data averaged over the zone provided by the TSO in a 15 minutes resolution. Then the RMSE is calculated, using the TSO measurement as verification. Except for the Tennet zone, the results are very similar for each forecast step. The RMSE for the inhomogeneous distributed and the homogeneous distributed approach are the same. Only the Tennet zone shows differences for the first forecast day (Figure 4).

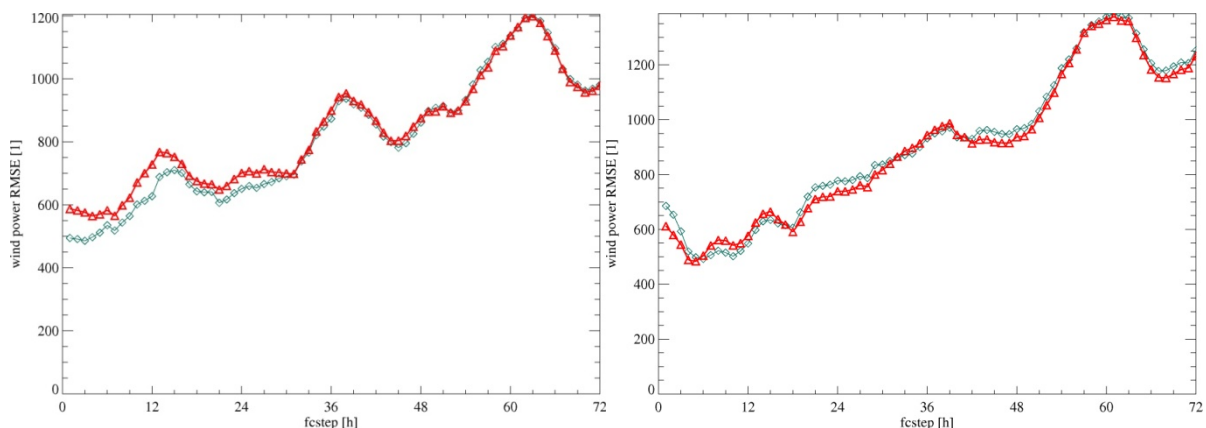


Figure 4: RMSE for the homogeneous distributed (red) and inhomogeneous distributed (green) approach for the Tennet zone (left) and the 50Hertz zone (right) in 2010.

For the first 24 forecast steps the inhomogeneous distributed approach has a smaller RMSE. For forecast days 2 and 3 the RMSE is the same for both approaches. Even though only the four German TSO zones are considered in this analysis, the results are promising. As the most interesting forecast horizon for future analysis is forecast day 2 and beyond, it is sufficient to assume a homogenous distribution of wind farm capacity.

3.2 European Error Maps

Based on the COSMO-EU data and a wind power conversion with the mean power curve assuming a homogenous wind farm distribution, forecast errors are calculated for every grid point. The following section presents the mean absolute error (MAE) and the RMSE on the European scale. The difference between these two statistical values lies mainly in the sensitivity towards outliers. The RMSE is more sensitive to the largest and smallest errors ([Wilks, 2011](#)). Besides the annual mean the statistical values are averaged over the different seasons to account for the strong seasonal variations in wind power production.

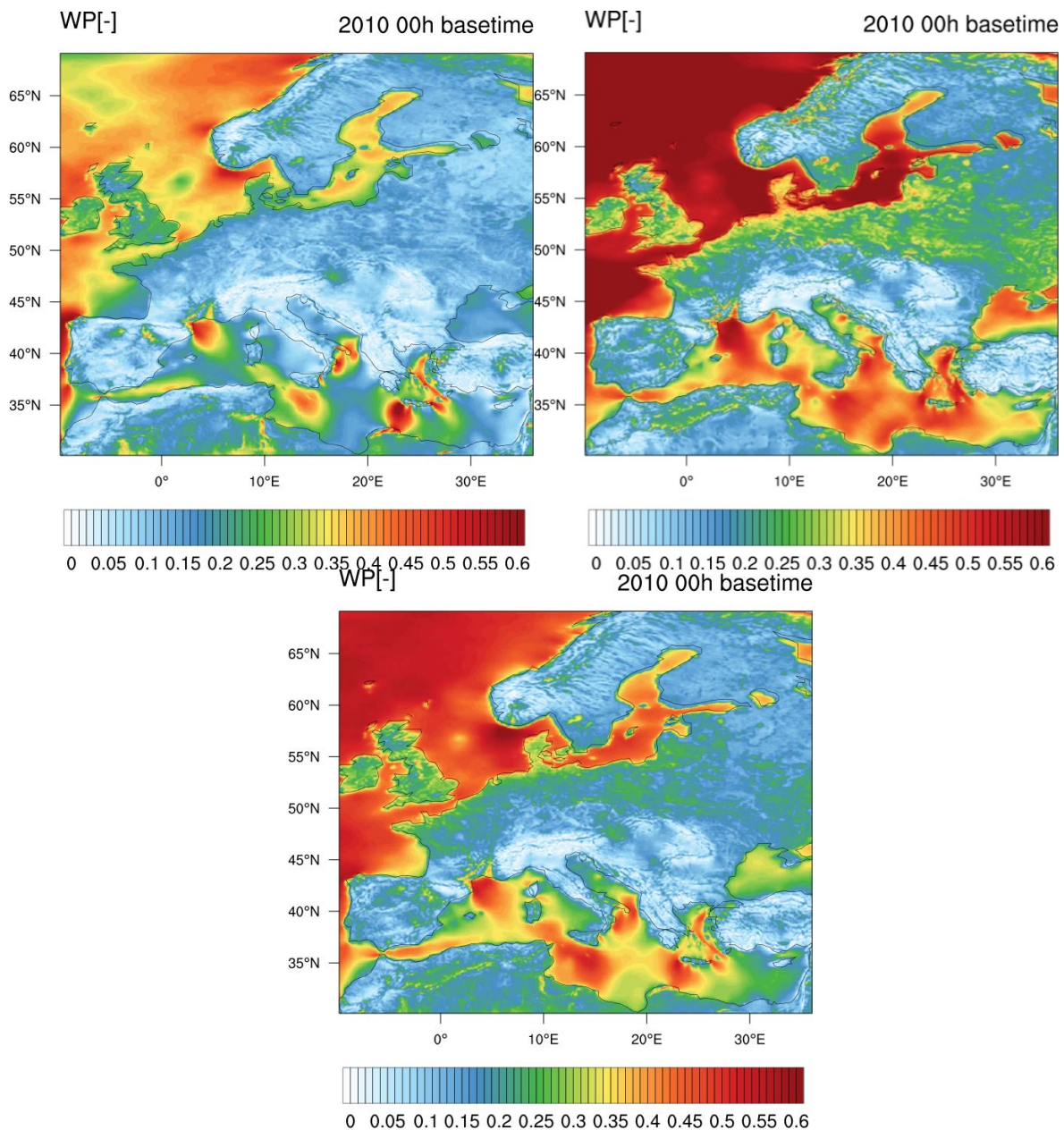


Figure 5: Mean produced wind power load factor for the summer season (top left), winter season (top right) and annual mean (bottom).

All wind power data is normalised with the load factor, which is the mean produced wind power. This kind of normalisation is reasonable ([Frias and Stoffels, 2012](#)) as it accounts for the higher wind power offshore. The annual averaged load factor and the summer and winter season averaged load factor can be seen in Figure 5. There is a significant difference between the small wind power production during summer and the large wind power production, especially offshore, during winter. Moreover local effects like the Mistral winds in Southern France or cut-off lows in the Mediterranean play an important role and result in high wind power during the year. Cut-off lows, also named cold air pool, are a meteorological phenomenon and the result of a polar belt trough in the upper-air flow extending down to the surface. The frequency of these phenomena was rather high in 2010 ([Wetterzentrale, 2012](#)). Especially the cut-off low is difficult to forecast. Hence, the forecast errors in the Mediterranean close to Southern Italy are high.

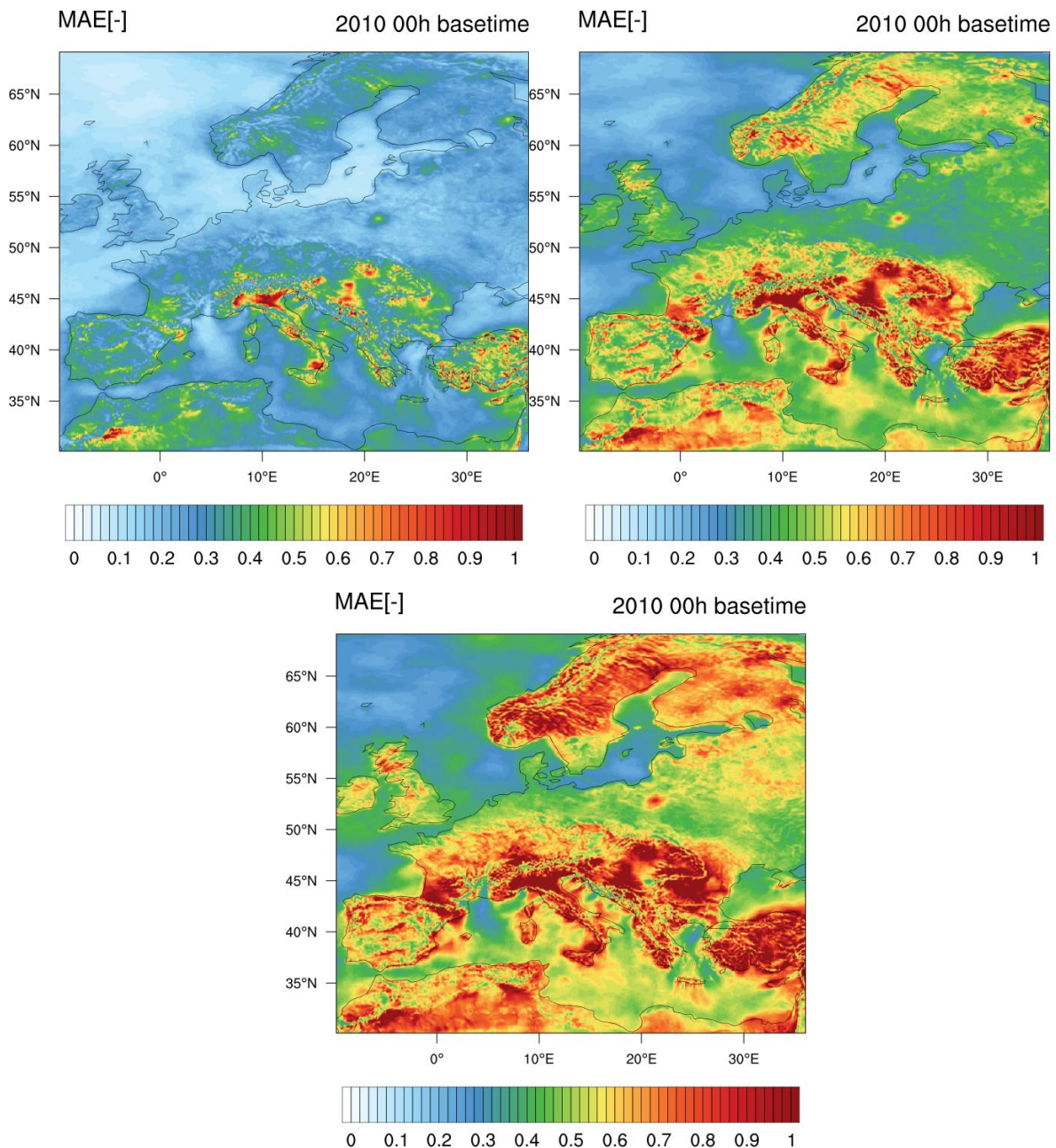


Figure 6: Mean absolute error averaged over 2010 for forecast day 1 (top left), forecast day 2 (top right) and forecast day 3 (bottom) normalised with the load factor.

Figure 6 shows the MAE averaged over 2010 for the different forecast horizons. Especially areas of complex terrain have a faster forecast error development than e. g. the northern offshore regions. In

the Mediterranean especially the cut-off lows lead to much larger forecast errors than in other offshore regions. In contrast to the cut-off lows the Mistral is well predictable.

For the first 24 hours the forecast errors are very small except for areas of very complex terrain. The largest forecast errors are reached there immediately. On day 3 even the coastal regions have high forecast errors and only few offshore regions have a small forecast error.

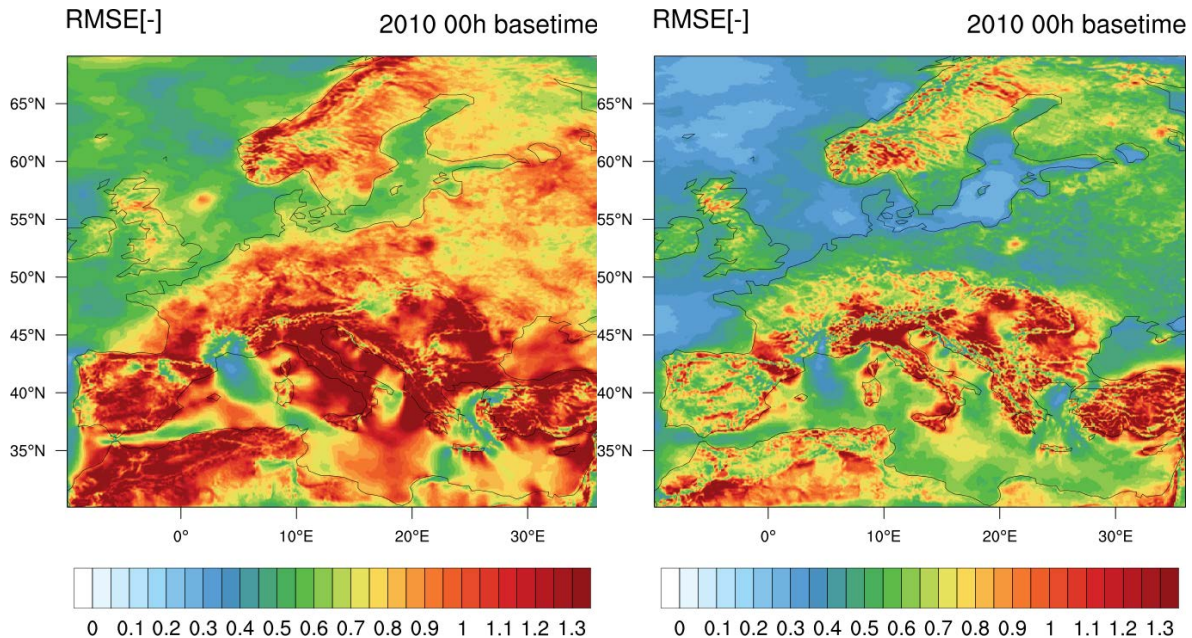


Figure 7: Root-mean-squared error for the summer season (left) and the winter season (right) for forecast day 2.

Figure 7 shows the seasonal RMSE for summer and winter for forecast day 2. The RMSE was chosen because it accounts better for large forecast errors and emphasizes the differences between the seasons. It becomes very clear, that during the summer period with smaller wind power output the relative forecast errors are much higher than during the winter season. Even the northern offshore regions have a high forecast error in summer with a focus on the centre of the North Sea. While the RMSE is also small for the complete German and Danish coast in winter, the same regions have very high errors in summer. Every site which has slightly complex terrain shows high error values in summer. One exception is once again the south of France, where the forecast errors in the Mistral region seem to be constantly small over the year. Moreover this region is characterised by high wind speeds and hence high wind power.

Single wind farm forecasts have high forecast errors. Pooling wind farms over a region, e. g. a TSO zone, helps to smooth out forecast errors ([Frias and Stoffels, 2012](#)). Therefore a smoothing of forecast error statistics was performed. The results are shown in Figure 8. On the left the smoothed yearly RMSE over a radius of 100 km is shown, on the right the 100 km smoothed MAE. Comparing the smoothed data to the grid based data (Figure 6), significant changes can be seen. In some regions the error could be reduced by 50 % (especially in more complex terrain). The coastal regions in Northern Germany still show a reduction of approximately 40 %.

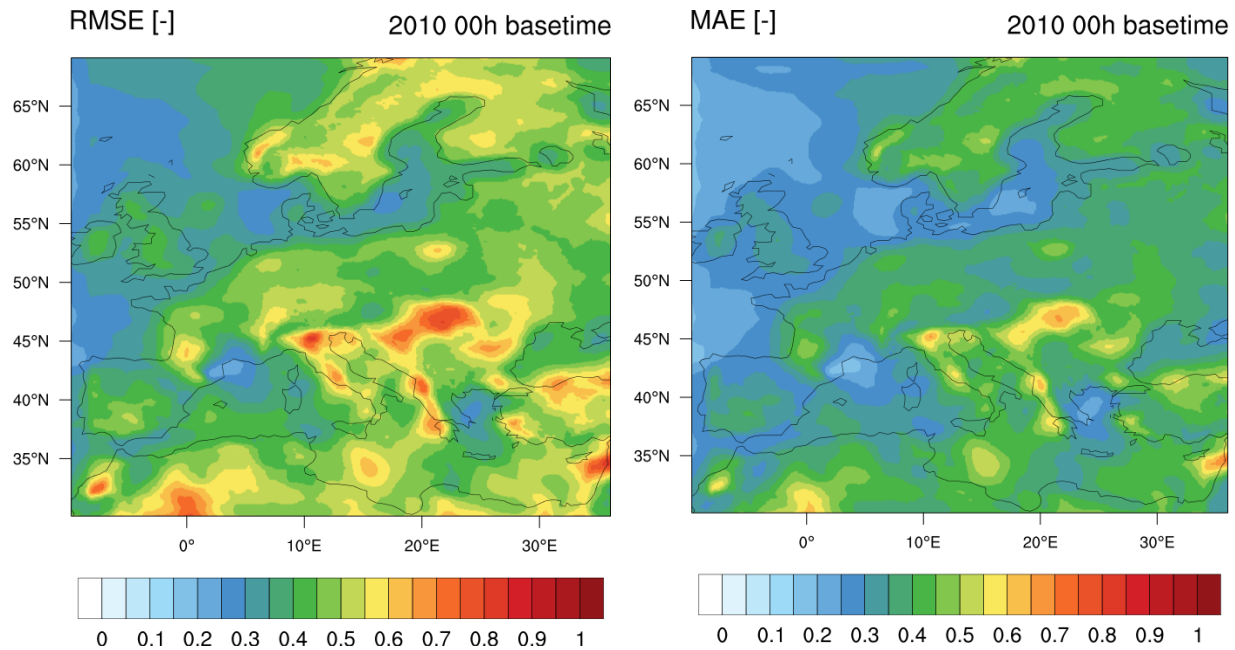


Figure 8: Smoothed RMSE (left) and smoothed MAE (right) both valid for forecast day 2, smoothed over a radius of 100 km, averaged over 2010 and normalised with the load factor.

3.3 Conclusions on large-scale predictability

Even though only the German TSO zones were analysed, using a limited period of one year, it became clear that, as long as the wind farms are rather equally distributed within the zone, it does not matter if the exact position of wind farms is considered in the wind power model or not. The resulting RMSE is the same. Even in the Tennet zone, where the majority of wind farms is concentrated in the northern part, the RMSE is the same from forecast day 2 on. As this forecast horizon is the interesting one, it is fair to assume homogenous distributed wind farms in Europe.

Considering wind power predictability in Europe, offshore wind power predictability outperforms onshore predictability with respect to the same energy yield. This is the case for the yearly averaged data as well as for the seasonal data. For onshore sites the predictability drops rapidly when the terrain is more complex. This makes especially the coastal regions favourable for wind energy development. Moreover local wind phenomena like the Mistral or a high frequency of cut-off lows have a significant impact on the produced wind power and the forecast errors. Hence, the forecast error maps display important additional information in terms of resource assessment and grid integration issues.

With regard to pooling wind farms, averaging over a region size of 100 km was performed as well. Thereby forecast errors are smoothed out significantly compared to the gridded data.

4. Wind Farm Predictability From Resource Assessment Campaigns

The development of a wind farm is grounded on the wind resource assessment phase where the developer determines the technical and economical feasibility of the project. To this end the developer carries out a site survey that includes a measurement campaign of at least one year. These measurements, combined with flow models and statistical tools, are used to design the wind farm layout and produce an estimate of the expected annual energy yield over a lifetime of 20 years. Then, the long-term wind energy production is the main input for a cost model that determines the economical feasibility of the project.

When evaluating the return of investment, the developer will primarily consider the prize of electricity expected in the next 20 years, something which depends on the regulatory framework of the electricity market. In countries like Spain, the wind farm operator is obliged to provide a day-ahead forecast of the energy production to help the TSO manage the power system. In a liberalised energy market, the market operator sets an hourly electricity price as well as imbalance tariffs for down and up-regulation. If the system, in a specific situation, requires up/down-regulation and the electricity producer is below/above the forecasted (traded) production, a penalization will be issued which is proportional to the deviation and the cost of regulating up/down. These penalties are naturally linked with the level of wind power predictability of the wind farm: the higher the predictability the lower the penalization and the faster the return of investment.

The question is: can we anticipate the economical impact of predictability during the planning phase in order to take it into account in the feasibility study of the wind farm? To answer this question it is necessary to develop a methodology that can make use of the available information of the site during the planning phase. The target variable is the predictability of the wind farm since this is ultimately linked with the trading benefits. Hence, an essential aspect of the study is to evaluate the methodology using onsite data from the both the planning and the operational phases.

The methodology will be explained with a case study comprising two Spanish wind farms. Due to confidentiality restrictions, the name and location of the wind farms will not be provided, although this information is not relevant for the analysis of the methodology or the results.

4.1 Methodology

The philosophy behind the method explained hereafter is to emulate the operational conditions with data from the resource assessment phase, since this allows direct use of wind power forecasting models and associated tools of the operational phase. To this end, the aim is to generate virtual time series of wind farm production upon which predictability is evaluated.

A wind farm model is built based on the WAsP wind atlas methodology ([Troen and Petersen, 1989](#)), the standard model used by the wind industry. WAsP flow model extrapolates the velocity from a reference mast (U_0) to the velocity at each turbine site at hub-height ($U_{hub,k}$, where k is the turbine index) by considering the topographic speed-up factors generated by terrain orography and roughness. Based on this velocity and the power curve provided by the manufacturer ($P(U_{hub})$) it is possible to extract the power output from each wind turbine position. Embedded in the WAsP package, the PARK model calculates the power losses due to wake effects within the wind farm. As a result, the model produces a collection of velocity ratios ($A_k = U_{hub,k}/U_0$) and wake efficiencies ($\eta_{wake,k}$) that depend on the wind speed and wind direction (φ_0) from the reference mast.

Then, the instantaneous wind farm power output is obtained by summation over the individual wind turbine power outputs:

$$P(t) = \sum_{k=1}^{N_{wt}} P_k(U_{hub,k}(t, \varphi_0)) \cdot \eta_{wake,k}(U_{hub,k}(t, \varphi_0)) \quad (1)$$

where N_{wt} is the number of wind turbines and the hub-height velocity is obtained from the velocity ratio:

$$A_k(\varphi_0) = \frac{U_{hub,k}}{U_0}(\varphi_0) \quad (2)$$

The method, when used for wind power forecasting is the core of the Prediktor model ([Landberg, 1999](#)), where the mast velocity is predicted by downscaling from a NWP using the geostrophic drag law.

The following assumptions are adopted in the wind farm model:

- i. All the wind turbine sites are immersed in the same wind climate regime, i.e. the correlation between the reference mast velocity and the turbine site velocity is close to one and all the wind turbines share the same wind direction sector observed by the met mast, i.e. $\varphi_k = \varphi_0$
- ii. The velocity ratios and wake efficiencies do not depend on the background stability of the atmosphere, i.e. neutral stratification assumed at all times
- iii. The flow is linearized, which means that the boundary layer is attached to the terrain regardless of the terrain complexity
- iv. The wind turbine response is determined by the manufacturer's power and thrust curves that are only a function of the hub-height wind speed, i.e. wind shear effects are not taken into account
- v. The wake model is analytic and does not include the interaction between wake and terrain, i.e. flat terrain is assumed in the wake model
- vi. Wake efficiencies are averaged values considering the wind speed distribution of each wind direction sector. Hence, the same wake efficiency is adopted regardless of the instantaneous wind speed
- vii. Electrical and availability energy losses are not included since this cannot be evaluated from the available data

In sites characterized by gentle slopes (below 30%) the linearized flow model works reasonably well, especially if the turbine site is exposed to similar terrain features than the reference mast site ([Bowen and Mortensen, 1996](#)). The assumption of uniform wind climate across the wind farm is also true if the wind farm extension is not very large (say less than 5 km) and the averaging time is long enough to filter out microscale turbulence (10 min to 1 hr).

In resource assessment studies the relevant variable is the annual energy production which is the result of averaging all wind climate conditions over a long term period. In this context, the prevailing wind condition dominates and positive and negative deviations from this mean state are cancelled out to some extent. This goes in favour of the assumption of neutral atmosphere which is the prevailing conditions in windy sites in onshore conditions. In offshore conditions or sites affected by strong diurnal temperature gradients (coast, mountains), non-neutral conditions can dominate the wind climate and larger errors from WAsP are expected.

The wake model is also built to produce averaged efficiencies over long-term periods. Then, when using the WAsP model to build virtual time series of wind power output, it is logical to expect important errors when the instantaneous conditions largely depart from the mean wind speed and/or the neutral atmosphere.

Based on this wind farm model and the met mast wind velocity and direction measurements, a virtual time series of wind farm production can be generated. Then, it can be used with a forecasting model to produce a time series of predicted wind farm production which is compared with the virtual production to extract a virtual wind power predictability. In the present study CENER's LocalPred deterministic forecasting model is used ([Martí et al., 2003](#)), based on NWP inputs, from the Skiron mesoscale model forced with GFS (Global Forecasting System) forecasts, and a MOS (Model Output Statistics) module that correlates them with wind farm production data.

Assuming that the interannual wind power predictability variations are not important, then one can expect that this virtual predictability will be similar during the lifetime of the wind farm. Then, the most important deviations between the predictability obtained in the planning and the operational phases will come from the differences between the virtual and the real wind energy production, which depends on the wind farm model performance.

The methodology adopted in this study can be easily assimilated by the wind energy industry since it is based on models that are widely used already in the resource assessment phase.

4.2 Case Studies

The case study comprises two wind farms in Spain, one in the North and one in the South. The characteristics of each wind farm are provided in Table 1. The available data corresponds to a year-long period in both the planning and the operational phase. The same annual period is used for the planning phase data, from September 2005 to August 2006, which consist on met mast velocity and direction measurements at various vertical levels. The operational phase period is based on data from 2008 for WF1 and 2011 for WF2. The data consists on observations from the scada system for the reference mast wind speed and direction at hub-height and wind farm power output. Hourly intervals are considered in both phases.

Table 1: Wind farms characteristics

Wind Farm ID	WF1	WF2
Region	North of Spain	South of Spain
Layout	(44x0.7 + 1x1.25)MW	14x2MW
Power [MW]	32.05	28
Rotor diameter [m]	48/62	70
Hub height [m]	45/62	84
Planning phase	01/09/05-31/08/06	01/09/05-31/08/06
<i>Mast levels [m]</i>	45, 20, 10	30, 15
Operational phase	01/01/08-31/12/08	01/01/11-31/12/11
<i>Mast levels [m]</i>	45	84

The orography and layout of the two sites are shown in Figure 9. WF2 is placed in fairly flat terrain and WF1 in a plateau delimited by slopes of 15-30%. The roughness length of both sites is uniform of 0.03 m. The reference met masts are placed in representative sites compared to the wind turbine positions and within a distance of 2 km.

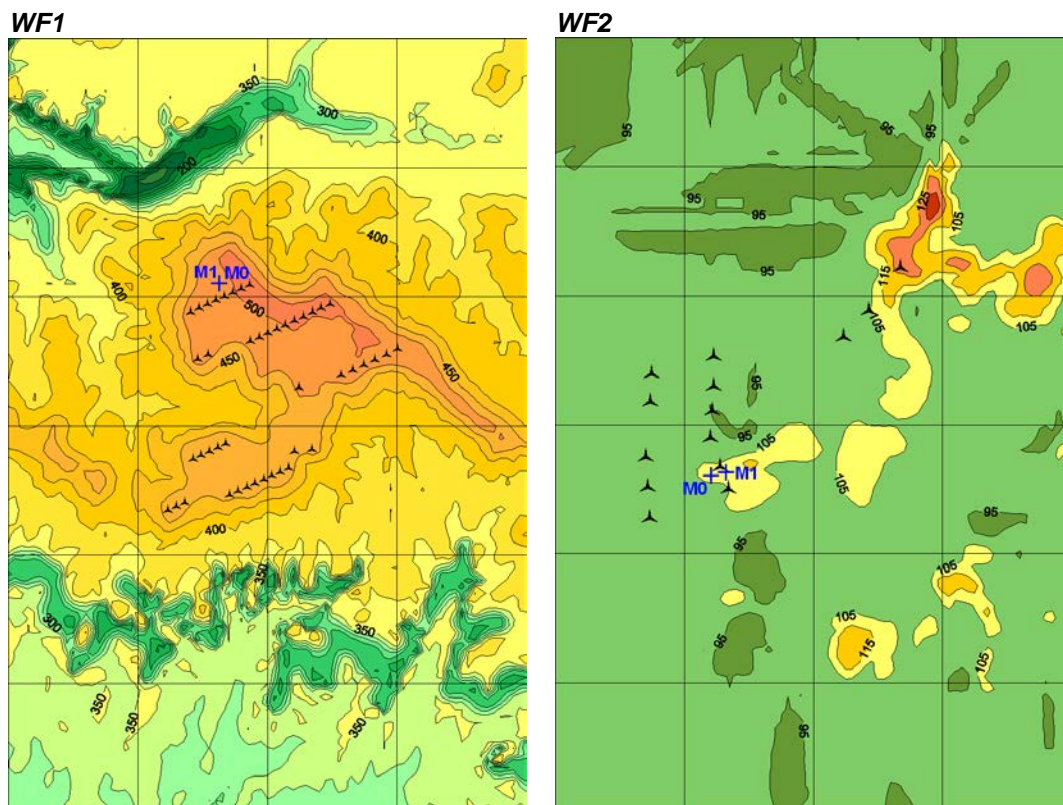


Figure 9: Maps and layouts of the two wind farms WF1 and WF2. M0 and M1 indicates the position of the reference mast in the planning and operational phases respectively. Elevation contours are provided every 25 m for WF1 and every 10 m for WF2

4.2.1 Wind climate changes between the planning and the operational phases

The interannual variations of predictability will depend on the variations of the wind climate (Weibull distribution and wind rose). Figure 10 shows the wind speed and direction distribution observed in the reference mast of both sites during the planning and the operational phases.

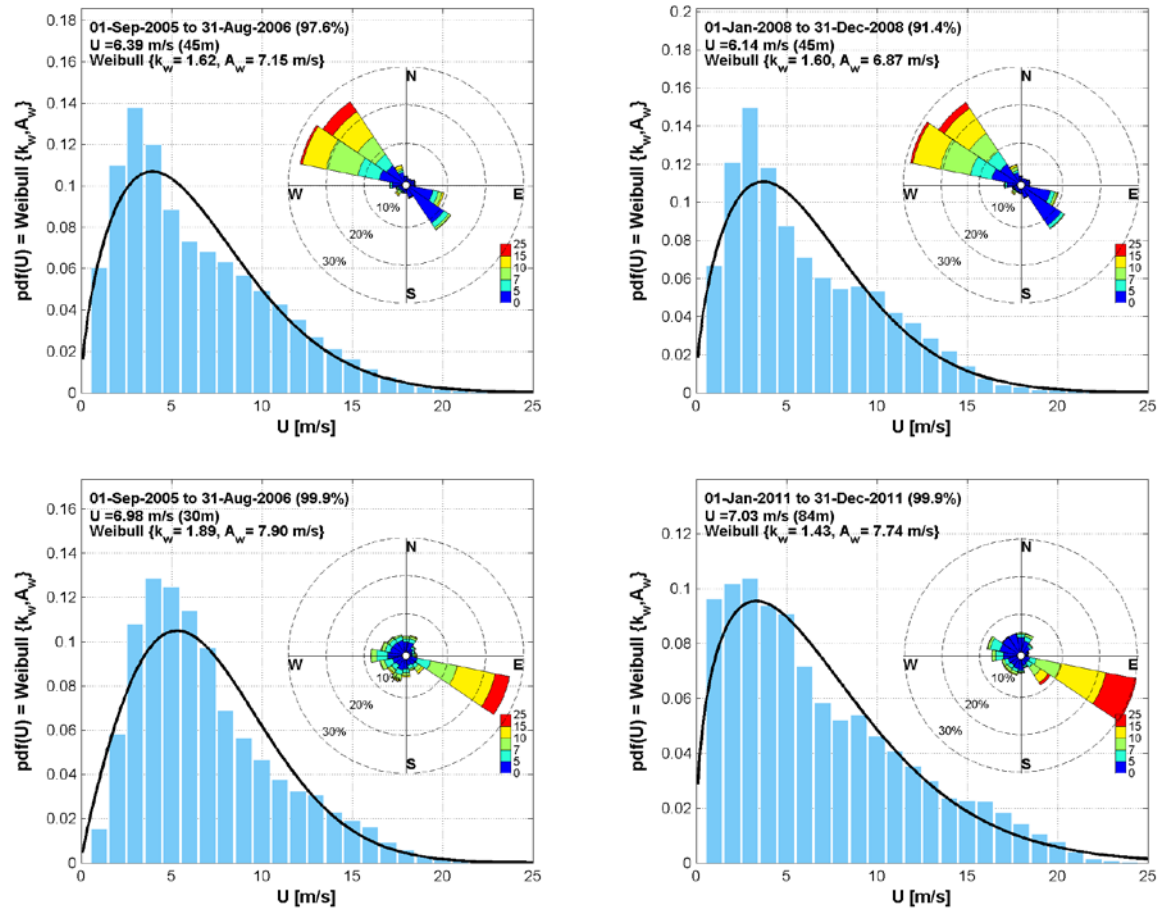


Figure 10: Annual wind velocity and direction distributions during the planning (left) and operational (right) phases for WF1 (top) and WF2 (bottom)

The following differences are noticed:

- **WF1:** The Weibull distribution is similar in both phases, composed of a mixed wind climate of dual distribution for low and high wind regimes. The windrose does not change since the prevailing wind sector is kept free of turbines in the operational phase. The annual mean wind speed at hub-height is reduced by 4% when moving from the planning phase to the operational phase.
- **WF2:** Large differences are observed in Weibull distribution with a much lower shape factor during the operational phase (heavier tail). The windrose shows the same prevailing sector from ESE but with higher intensity in the operational phase. Such an important change in the wind climate cannot be attributed to the presence of nearby wind turbines or the difference in sensor height. It is rather due to a notable change in the synoptic activity of the region which is dominated by the large-scale channelling through the Strait of Gibraltar. As a result the annual mean wind speed at hub-height is reduced by as much as 14.3% when moving from the planning phase to the operational phase.

Hence, both sites are good examples of the situations that can happen when moving from the planning to the operational phase: while WF1 shows consistent wind climates in the two phases WF2 shows a significant change of wind climate due to large interannual variability of the synoptic activity of the region.

4.3 Model evaluation

4.3.1 Planning phase

In the absence of multiple met masts for an evaluation of the flow model performance across the site, model evaluation is based on self-prediction of the mean wind profile at the reference mast. Table 2 shows the observed and predicted mean velocity and wind shear. The normalized bias is calculated as the difference between predicted and observed mean values divided by observed mean.

Table 2: Self-prediction of mean wind profile. U_m and U_w are the measured and predicted mean velocity, z is the height above ground level and α is the power-law exponent indicative of the wind shear

WF1	z [m]	U_m [m/s]	U_w [m/s]	NBIAS [%]
	10	5.55	5.36	-3.5
	20	6.14	5.74	-6.5
	45	6.39	6.34	-0.9
	$\alpha(10/20)$	0.14	0.10	-31.4
	$\alpha(20/45)$	0.05	0.07	41.3
WF2	z [m]	U_m [m/s]	U_w [m/s]	NBIAS [%]
	15	6.29	6.28	-0.2
	30	6.97	6.94	-0.5
	$\alpha(15/30)$	0.15	0.14	-2.6

The wind profile is correctly reproduced by WAsP in WF2 with errors below 1%. With this good performance it is reasonably to assume that the model will also produce good estimates when extrapolating vertically from the upper level of the mast to hub-height.

On the other hand, large errors are observed in WF1 due to the difficulties in simulating the flow at the edge of the plateau in the prevailing wind direction from NW. Nevertheless, the upper velocity level is situated already at hub-height and therefore the model does not need to extrapolate vertically.

4.3.2 Operational phase

The performance of the wind farm model can be assessed during the operational phase by comparing the time series of virtual and real production. Table 3 shows the annual errors of both wind farms. The error is normalized by dividing with the total installed capacity of the wind farm. Performance indicators typically used in deterministic wind power forecasting are also used here ([Madsen et al., 2005](#)).

Table 3: Performance of the wind farm model

	WF1	WF2
NBIAS [%]	-2.8	-1.5
NMAE [%]	7.7	6.4
NRMSE [%]	12.4	11.5

The model shows some underprediction of the annual production at both sites although the general performance is fairly good. Notice that the underprediction could have been larger if electrical and availability losses would have been included in the wind farm model. Nevertheless, the error level is similar in the three cases with a variability band of only 1.5% in the NMAE. The largest error is observed in WF1 due to the poorer performance of the flow model and a more significant contribution of wake effects.

Figure 11 shows the evolution of the modelling error by month and by wind direction sector. The seasonal evolution of the error in WF1 and WF2 is similar since both sites are located in the same region. It is observed that the seasonal variability of the NMAE is within a 5% band.

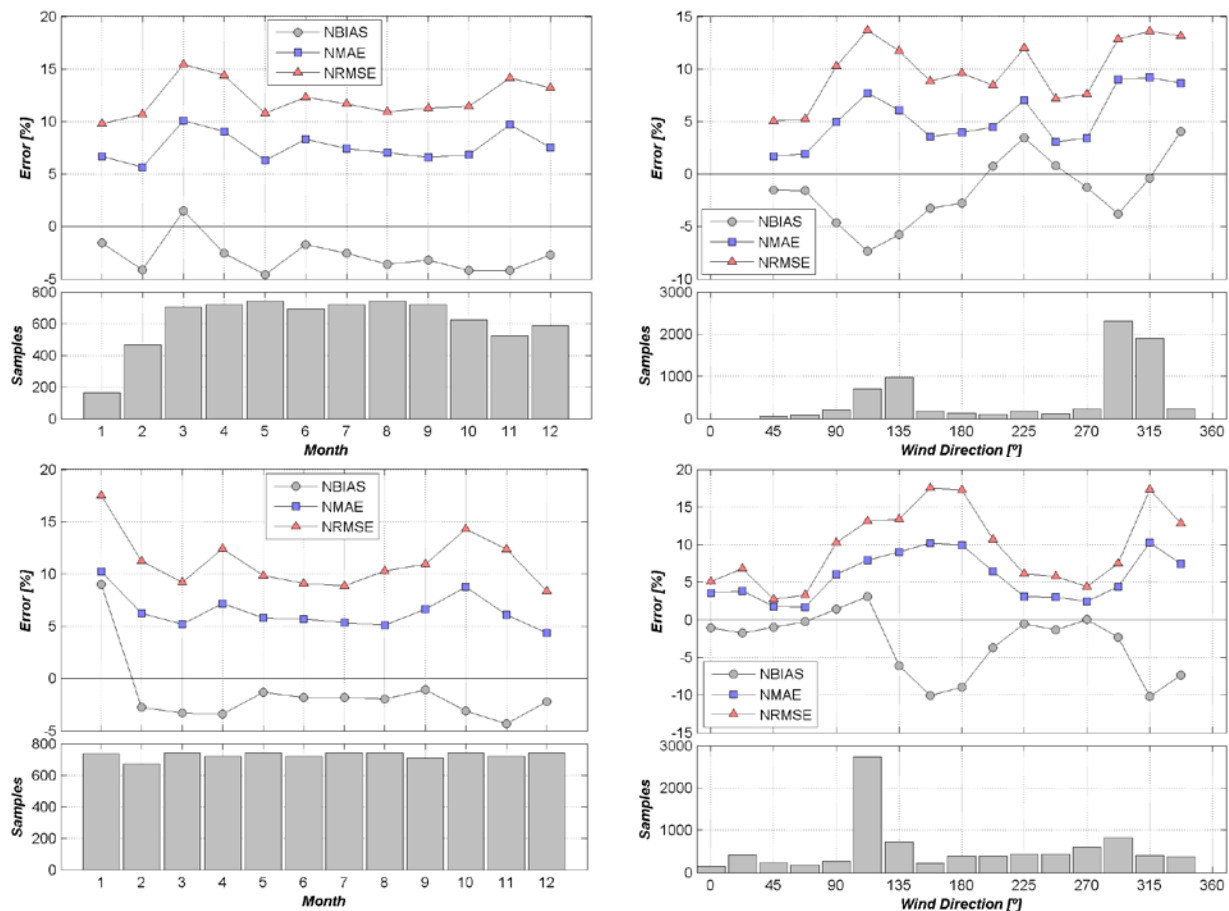


Figure 11: Monthly (left) and sector-wise (right) normalized errors between the virtual and the real time series of wind energy production during the operational phase for WF1 (top) and WF2 (bottom)

Considering the dependency of the model error with the wind direction, it is observed that the error peaks where the wake effects are the largest.

4.4 Predictability assessment

LocalPred wind power forecasting model is run on the real and virtual time series of wind power production data to evaluate predictability. To this end, the model is trained using the first 6 months of data and then the evaluation is performed using the remaining 6 months of each period. The forecasting model is run for a 72-hr long prediction which is initialized every day at 12h UTC.

Figure 12 and Figure 13 show the dependency of the forecasting errors with the look-ahead time for WF1 and WF2 respectively. The errors from the real production data are compared with those obtained from the virtual production data from the planning and operational phases.

Daily cycles of the errors are observed since the forecasting model is initialized once a day allowing for the highlighting of the intraday error variability of the GFS input data. These cycles are quite repeatable from year to year in WF1 as a result of the similitude of wind climate observed between the planning and operational phases. This is not the case in WF2 where a distinct daily pattern is observed in both phases.

Despite of the larger wind climate variability observed in WF2, predictability is higher due to the much simpler local topography which results in higher performance of the mesoscale model. The error growth is also less pronounced in WF2.

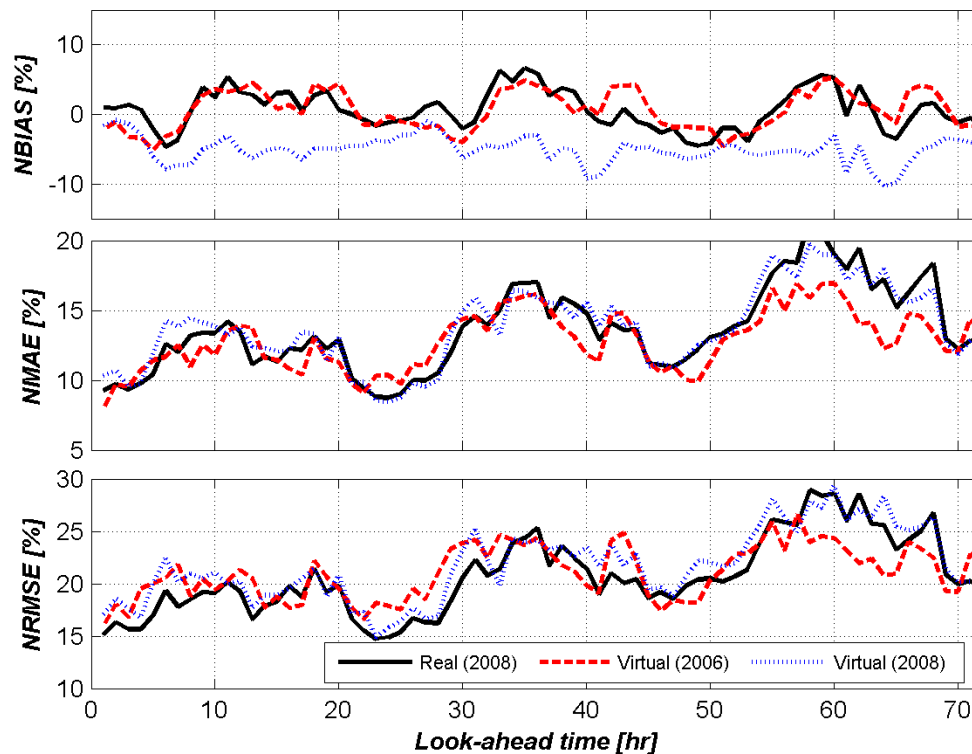


Figure 12: Wind power forecasting error versus look-ahead time for a 72-hr horizon range for WF1. The predictability from the "real" operational production data is compared with the predictability from the "virtual" production data generated from the wind speed measurements during the planning (2006) and operational (2008) phases

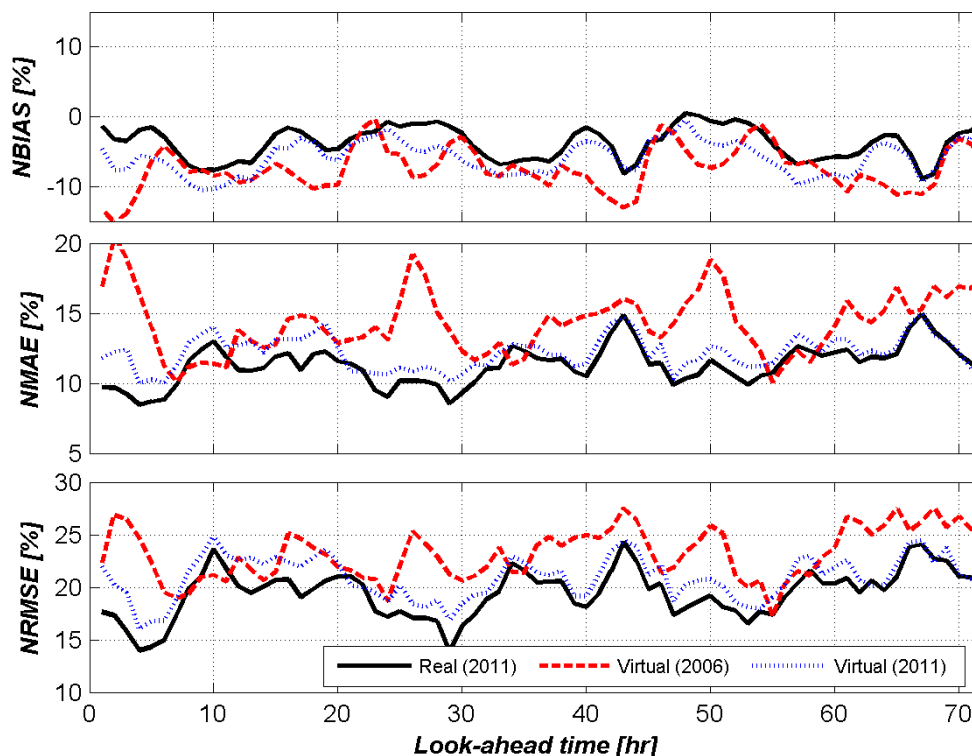


Figure 13: Wind power forecasting error versus look-ahead time for a 72-hr horizon range for WF2. The predictability from the "real" operational production data is compared with the predictability from the "virtual" production data generated from the wind speed measurements during the planning (2006) and operational (2011) phases

In the context of predictability assessment we shall focus on mean errors over a given prediction horizon. Table 4 shows mean errors for the first three days of prediction. The NBIAS show more scatter in the results owing to the inherent error compensation of this indicator. In the case of WF1 the differences between the virtual and the real NMAE/NRMSE in the first two days of prediction is within 0.2/1.3% and 0.5/1.3% from the planning and operational phases respectively. The corresponding differences for WF2 are 3.2/4.3% and 1.4/2.1%, larger than WF1 due to the large differences in wind climate observed in WF2. Further work should be conducted to have a better assessment of the interannual variability of the predictability level.

Table 4: Mean daily forecasting errors from the real and virtual time series of wind power production data for WF1 and WF2

	WF1			WF2		
	Real (2008)	Virtual (2006)	Virtual (2008)	Real (2011)	Virtual (2006)	Virtual (2011)
NBIAS [%]						
0-24 hr	0.9	0.5	-4.7	-3.9	-8.1	-6.3
24-48 hr	0.9	0.7	-4.9	-3.7	-7.4	-5.5
48-72 hr	0.0	0.5	-5.7	-3.8	-7.0	-5.8
NMAE [%]						
0-24 hr	11.4	11.2	11.9	10.7	13.7	12.2
24-48 hr	13.3	13.1	13.4	11.2	14.3	11.9
48-72 hr	16.1	14.0	15.9	11.9	14.9	12.5
NRMSE [%]						
0-24 hr	17.8	19.1	19.0	19.0	22.1	21.0
24-48 hr	20.3	21.5	21.4	19.2	23.4	20.6
48-72 hr	24.0	22.5	24.7	20.1	24.1	21.1

4.5 Conclusions on local-scale predictability

Assessing the impact of predictability during the planning phase is feasible using wind farm models that are already widely used for wind resource assessment studies. Combined with state-of-the-art forecasting models, it is possible to produce predictability information.

Two sites have been studied with different wind climates and terrain complexities. For long-term assessment studies it is necessary to take into account the interannual variability of the wind climate considering its impact on the wind resource and predictability levels. In the case of a moderate change of interannual wind climate predictability can be anticipated quite accurately with deviations of less than 0.5% in the NMAE. In the case of a large interannual variability deviations in predictability assessment will be more important, in this case around 3% deviation in NMAE when the annual wind speed changed by 14.3% between planning and the operational phases. The only way to minimize these deviations is to increase the length of the reference period such that a larger portion of the climatic variability is characterized and taken into account.

This methodology can be used to emulate the trading of the annual energy production in the electricity market and get an early estimate of the penalties that the wind farm will receive due to the lack of predictability. The predictability level is itself also an indicator of quality-of-energy for grid integration purposes. Hence it is worth including such parameter in the planning phase of a wind farm.

5. Guidelines for End-Users

This report summarizes the first approaches towards producing wind power predictability assessments during the planning phase of wind energy. To this end, two scales have been analyzed corresponding to typical end-user scenarios: the large European scale and the local wind farm scale. The following conclusions and guidelines can be extracted from these preliminary studies:

- Studying wind power predictability during the planning phase is feasible and advantageous
- The same wind farm models of standard use in wind resource assessment can be applied to generate virtual time series of wind power output and emulate operational conditions in hindcast mode, making use of historical records of wind speed
- Concerning wind power predictability in Europe, offshore wind power predictability outperforms onshore predictability with respect to the same energy yield
- For onshore sites the predictability drops rapidly when the terrain is more complex. This makes especially the coastal regions favourable for wind energy development
- Especially complex terrain areas profit from aggregation of several wind farms by forecast error smoothing. Forecast errors in these areas can be reduced up to 60 %
- Additionally to the capacity factor at sites, a combination of the forecast error, the smoothing factor and the spatial correlation of wind speed can complement feasibility studies by adding information about the quality of the wind for integration purposes

6. References

- Bowen AJ, Mortensen NG (1996) Exploring the limits of WAsP The Wind Atlas and Application Program. Proceedings of EWEC-96, Göteborg, Sweden, May 1996
- COSMO [Online]. - 10 04, 2011. - 11 10, 2011. - <http://www.cosmo-model.org/>.
- EWEA, (2009) Integrating Wind, Developing Europe's power market for the large-scale integration of wind power. TradeWind Final Report, 2nd edition, May 2009, pp 102
- Focken U, Lange M, Mönnich K, Waldl H-P, Beyer HG, Luig A (2002) Short-term prediction of the aggregated power output of wind farms e a statistical analysis of the reduction of the prediction error by spatial smoothing effects. *J. Wind Eng. Ind. Aerodyn.* **90**: 231-246.
- Foley AM, Leahy PG, Marvuglia A, McKeogh EJ (2012) Current methods and advances in forecasting of wind power generation, *Renewable Energy* **37**: 1-8
- Frias L, Stoffels N (2012) Statistical analysis of wind power and prediction errors for selected test areas. Deliverable D7.1 of the FP7-Safewind project, grant number 213740, 27 pp
- Giebel G, Brownsword R, Kariniotakis G, Denhard M, Draxl C (2011) The State-Of-The-Art in Short-Term Prediction of Wind Power. A Literature Overview, 2nd Edition. Deliverable D1.2 of the FP7-ANEMOS.plus project, grant number 038692, 109 pp
- Giebel G, Kariniotakis G (2011) Best Practice in the Use of Short-term Forecasting of Wind Power. Guidelines and Recommendations for End Users. Deliverable D6.3 of the FP7-ANEMOS.plus project, grant number 038692, 13 pp
- Landberg L (1999) Short-term Prediction of the Power Production from Wind Farms. *J. Wind Eng. Ind. Aerodyn.* **80**: 207-220
- Madsen H, et al. (2005) Standardizing the Performance of Short-Term Wind Prediction Models, *Wind Engineering* **29**: 475-489
- Martí I, Usaola J, et al. (2003) Wind power prediction in complex terrain. LocalPred and Sipreólico. Proceedings of EWEC-03, Madrid, Spain June 2003.
- McLean JR (2008) Equivalent Wind Power Curves. Deliverable D2.4. of FP7-TradeWind project, grant number EIE/06/022/SI2.442659
- Rombauts Y, Delarue E, D'haeseleer E (2011) Optimal portfolio-theory-based allocation of wind power: Taking into account cross-border transmission-capacity constraints. *Renewable Energy* **36**: 2374-2387
- Troen I, Petersen EL (1989) European Wind Atlas. Risø National Laboratory, Roskilde. ISBN 87-550-1482-8. 656 pp
- Wetterzentrale [Online]. - 09. 03 2012. - <http://www.wetterzentrale.de/topkarten/tknav.html>.
- Wilks DS (2011) Statistical Methods in the Atmospheric Sciences. Oxford Academic Press, Vol. International Geophysics Series